Renewable Energy, Environment, and Power Quality Journal (REE&PQJ)
ISSN:3020-531X
Volume 26, July 2026

NSGA-II Optimization Framework for Multi-Criteria Individual Pitch Control Design in Floating Offshore Wind Turbines

Lei Ren[1], Matilde Santos[2], Xin Cai[1] and J. Enrique Sierra-Garcia[3]

[1] College of Mechanics and Engineering Science, Hohai University
Nanjing, 211100(China), RyanL177@outlook.com, xcai@hhu.edu.cn
[2] Institute of Knowledge Technology, Complutense University of Madrid
Madrid 28040(Spain), msantos@ucm.es
[3] Systems Engineering and Automation, University of Burgos, Burgos 09004(Spain), jesierra@ubu.es

Abstract. The effective implementation of Individual Pitch Control (IPC) is crucial for mitigating structural loads and platform motions in floating offshore wind turbines (FOWTs), yet the tuning of its controller parameters presents a complex multi-objective challenge. This study proposes a systematic optimization framework to address this issue. A multi-objective optimization problem is formulated with the goal of simultaneously minimizing blade root fatigue loads, power fluctuations, and pitch actuator duty. The Non-dominated Sorting Genetic Algorithm II (NSGA-II) is employed to identify the Pareto-optimal set of proportional-integral (PI) gains for the IPC system. Time-domain simulations of a reference FOWT model demonstrate that all optimized control strategies significantly outperform conventional collective pitch control, achieving a reduction of up to 27.6% in blade root load fluctuations and improved platform stability. Among them, the balanced strategy derived from the Pareto front offers the most favourable overall trade-off, providing substantial load reduction with reasonable actuator activity. The results validate the proposed framework as an effective tool for the design of high-performance IPC systems for FOWTs.

Key words. Floating Offshore Wind Turbines, Individual Pitch Control, Multi-Objective Optimization, NSGA-II, Pareto front, Load Reduction

1. Introduction

In modern wind turbine control systems, pitch control plays a critical role in optimizing power output and mitigating structural loads. Traditional collective pitch control (CPC) adjusts all blades simultaneously based on rotor speed error, typically using Proportional-Integral (PI) controllers with gain scheduling to handle system nonlinearities [1]. While CPC is effective in regulating generator speed and maintaining rated power in above-rated wind conditions, it assumes uniform aerodynamic loads across all blades—a condition rarely met in real-world environments due to wind shear, turbulence, and atmospheric inhomogeneity. This limitation leads to unbalanced rotor loads, increased fatigue, and potential structural failures, especially in large-scale turbines.

The challenges of CPC become more pronounced in floating offshore wind turbines (FOWTs), where additional complexities such as platform motions, wave-induced vibrations, and wind-wave coupling exacerbate load asymmetries and system dynamics. For instance, semi-submersible FOWTs experience significant low-frequency vibrations and 1P oscillations in the blade root bending moment, which CPC cannot address effectively due to its inherent design [2]. The classic and most widely implemented IPC architecture involves separate PI controllers for the tilt and yaw moments, which are derived from the blade root bending moments through a multi-blade coordinate (MBC) transformation.

To overcome these limitations, individual pitch control (IPC) has emerged as an advanced solution. Unlike CPC, IPC independently adjusts the pitch angle of each blade based on localized load measurements, enabling targeted mitigation of asymmetric loads and platform-induced vibrations. Studies demonstrate that IPC significantly reduces periodic loads in key components such as the blades, tower, and hub. Namik et al. [3] showed through high-fidelity simulations that IPC can achieve substantial reductions of 44% in power fluctuation, 39% in platform rolling rate, and 43% in pitching rate compared to conventional controllers.

Despite its proven benefits, the performance of this standard IPC structure is highly dependent on the precise tuning of its PI controller parameters (K_p and K_i). Suboptimal gains can lead to inadequate load reduction, excessive pitch actuator usage, or even system instability. Therefore, there remains a persistent need and significant value in improving the core PI control loop of IPC. A robustly tuned and optimized set of IPC PI gains can deliver substantial performance benefits with a simple, reliable controller structure. The optimization of IPC's PI gains is inherently a multi-objective problem, aiming to simultaneously maximize load reduction and minimize pitch actuator activity. To solve such problems, the wind energy field has seen the application of various metaheuristic algorithms, including swarm intelligence-based methods like Multi-Objective Particle Swarm Optimization (MOPSO)[4] and physics-inspired algorithms like the Archimedes Optimization Algorithm (AOA) [5], the latter having been used for pitch controller tuning. Among these, the Non-dominated Sorting Genetic Algorithm II (NSGA-II) is a prominent evolutionary multi-objective algorithm frequently employed in wind energy studies for tasks ranging from wind turbine layout to aerodynamic design[6], [7]. Its selection for this work is justified by its proven capability to maintain solution diversity and generate well-distributed Pareto frontiers, which is essential for exploring the trade-offs between competing control objectives effectively. Therefore, this work focuses on the fundamental optimization of the PI controller gains (K_p and K_i) for IPC using NSGA-II, aiming to enhance load reduction performance in FOWTs.

2. Methodology

A. Reference Wind Turbine and Platform Model

The configuration of the International Energy Agency (IEA) 15MW offshore reference wind turbine with the VolturnUS-S semi-submersible platform is studied in this research [8], as shown in Fig. 1.

The IEA 15 MW offshore wind turbine, featuring three upwind blades, is installed on the VolturnUS-S semi-submersible platform. Table I provides the main specifications of the wind turbine, with SWL denoting the still water level. The wind turbine blades are treated as rigid, while tower flexibility is taken into account. The reference platform presented in this research is a three-column, steel semisubmersible.

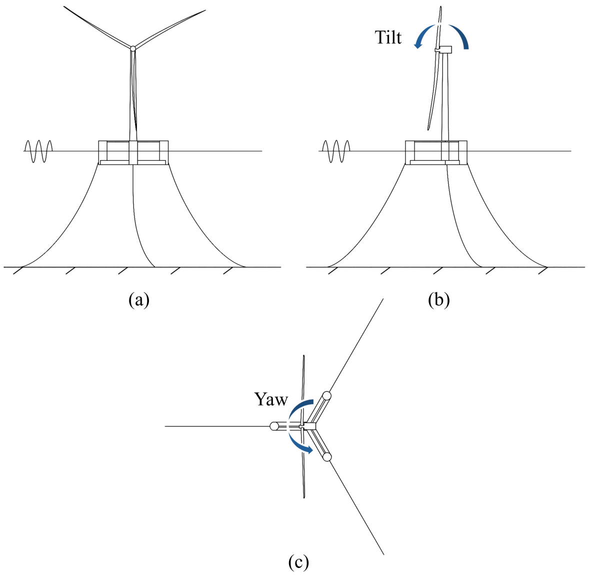

Fig. 1 IEA 15MW offshore reference wind turbine with the VolturnUS-S semi-submersible platform (a) front view; (b) side view with tilt direction; (c) top view with yaw direction.

Table I. - Wind turbine information and parameters

PARAMETERS	VALUE
Rotor type	Upwind, 3 Blades
Rated Power	15 MW
Rotor diameter	240 m
Hub height above SWL	150 m
Cut-in wind speed	3 m/s
Rated wind speed	10.59 m/s
Cut-out wind speed	25 m/s
Minimum rotor speed	5.0 m/s
Maximum rotor speed	7.56 m/s

B. Individual Pitch Control Design

In large three-bladed wind turbines, the non-uniform distribution of aerodynamic loads—particularly the 1P harmonic loads induced by factors such as wind shear and tower shadow effects—is a key factor leading to blade fatigue damage. To mitigate such loads, Individual Pitch Control (IPC) achieves dynamic load balancing by applying differentiated pitch commands to each blade. However, the blade dynamics in the rotating coordinate system exhibit strong coupling and periodic time-varying characteristics, making direct controller design highly complex. Therefore, the Multiblade Coordinate Transformation (MBC) [9] is employed to convert the rotating-frame dynamics into a fixed coordinate system for linearization, providing a suitable control framework for IPC.

MBC is a mathematical transformation based on the blade azimuth angles ψ_i, with its core function being to decouple periodic signals in the rotating coordinate system. Through the MBC transformation, the blade loads (bending moments) in the rotating coordinate system are converted into two components in the non-rotating coordinate system: the tilt moment M_t(t) and the yaw moment M_y(t), the corresponding directions are shown in Fig. 1. In the MBC transformation targeting the 1P harmonic, the out-of-plane (OoP) bending moments of the three blades — defined as the moment component normal to the rotor plane — form a vector M(t) = $[M_1(t)\ M_2(t)\ M_3(t)]^T$. This vector is input into the forward MBC transformation matrix $T(\psi)$ to compute the azimuth-independent moment components M_t(t) and M_y(t) in the fixed coordinate system. Their relationship is given as follows:

$$\begin{bmatrix} M_t(t) \\ M_y(t) \end{bmatrix} = T(\psi) M(t) \tag{1}$$

where, the three-element vector ψ contains the azimuth angles of each blade (with the vertical upward position of the blade defined as zero degrees). The forward transformation matrix is given by:

$$T(\psi) = \frac{2}{3} \begin{bmatrix} \cos(\psi_1) & \cos(\psi_2) & \cos(\psi_3) \\ \sin(\psi_1) & \sin(\psi_2) & \sin(\psi_3) \end{bmatrix} \tag{2}$$

Subsequently, to suppress the M_t and M_y components, the corresponding tilt pitch angle β_t(t) and yaw pitch angle β_y(t) are typically computed within the IPC control module through decentralized control. Then, these two pitch signals in the fixed coordinate system are converted back to the rotating coordinate system via the inverse MBC transformation to obtain the IPC components in the rotating coordinate system:

$$\begin{bmatrix} \beta_{IPC1}(t) \\ \beta_{IPC2}(t) \\ \beta_{IPC3}(t) \end{bmatrix} = T^{-1}(\psi + \psi_0) \begin{bmatrix} \beta_t(t) \\ \beta_y(t) \end{bmatrix} \tag{3}$$

The inverse transformation matrix T^{-1} is given by the formula:

$$T^{-1} = \begin{bmatrix} \cos(\psi_1 + \psi_0) & \sin(\psi_1 + \psi_0) \\ \cos(\psi_2 + \psi_0) & \sin(\psi_2 + \psi_0) \\ \cos(\psi_3 + \psi_0) & \sin(\psi_3 + \psi_0) \end{bmatrix} \tag{4}$$

The parameter ψ_0 is the azimuth offset, used to effectively reduce the residual coupling effects between the two components in the fixed coordinate system. Finally, the IPC components for each blade $\beta_{IPC,i}(t)$ are superimposed with the Collective Pitch Control (CPC) signal $\beta_{CPC}(t)$ to calculate the pitch command value $\beta_i(t)$ for each blade.

$$\beta_i(t) = \beta_{CPC}(t) + \beta_{IPC,i}(t) \tag{5}$$

where $\beta_{CPC}(t)$ is generated based on the wind turbine's average wind speed, with the primary objective of maintaining rated power. In contrast, $\beta_{IPC,i}(t)$ aims to suppress periodic unbalanced loads induced by effects such as wind shear and tower shadow.

The $\beta_{CPC}(t)$ is typically produced by a PI controller acting on the rotor speed error. Its control law is given by:

$$\beta_{CPC}(t) = K_{p,cpc} e_{CPC}(t) + K_{i,cpc} \int e_{CPC}(t)dt \tag{6}$$

where $e_{CPC}(t)$ is the deviation of rotor speed from its nominal value, $K_{p,cpc}$ and $K_{i,cpc}$ are the proportional and integral gains of the *CPC* controller, respectively.

In the fixed coordinate system, two separate PI controllers are designed to suppress the tilt moment $M_{t(t)}$ and the yaw moment $M_{y(t)}$, producing the corresponding tilt pitch command β_t(t) and yaw pitch command β_y(t). For the tilt channel, the control law is:

$$\beta_t(t) = K_p e_t(t) + K_i \int e_t(t)dt \tag{7}$$

where $e_t(t) = M_{t,ref} - M_{t,t}$ and the setpoint is typically $M_{t,ref} = 0$ for load minimization. The yaw channel β_y(t) follows the identical PI control law and shares the same controller parameters; it uses its own error signal $e_y(t)$ but the same proportional gain K_p and integral gain K_i.

The fixed-frame pitch commands β_t(t) and β_y(t) are then transformed back into the rotating frame via the inverse MBC transformantion given in Eqs. (3) and (4), yielding the three IPC components [$\beta_{IPC1}(t)$, $\beta_{IPC2}(t)$, $\beta_{IPC3}(t)$].

C. Multi-objective Optimization Problem Formulation

The multi-objective optimization problem for IPC PI controller tuning is mathematically formulated to simultaneously minimize three conflicting performance metrics that represent the key trade-offs in wind turbine control design.

The CPC controller gains in Eq. (6) are predefined via gain-scheduling and are not optimized here. The decision variables are the proportional K_p and integral gains K_i of the IPC controller for the 1P load component, which are common to both the tilt and yaw channels as described in Eq.(7):

$$x = [K_p \quad K_i]^T \tag{8}$$

where the search space is constrained by bounds determined through prior sensitivity analysis:

$$\begin{aligned} K_p &\in [1\times10^{-10},\ 1\times10^{-8}] \\ K_i &\in [1\times10^{-11},\ 1\times10^{-9}] \end{aligned} \tag{9}$$

Three objective functions are defined to be minimized:

$$\begin{aligned} f_1(x) &= DEL_{rootMOoP1} \\ f_2(x) &= \sigma_{power} \\ f_3(x) &= \sigma_{pitch\_rate} \end{aligned} \tag{10}$$

The Damage Equivalent Load (DEL) of the blade root out-of-plane bending moment is calculated using rainflow counting [10] to extract load cycles from the time series data. The DEL is derived according to the Palmgren-Miner linear damage accumulation rule [11]:

$$DEL = \left(\frac{\sum_{i=1}^{k} (n_i \cdot S_i)}{N_{eq}} \right)^{\frac{1}{m}} \tag{11}$$

where n_i is the number of cycles at stress range S_i obtained from rainflow counting, m is the Wöhler (S-N) curve exponent and N_{eq} is the reference number of cycles. The standard deviation of the generator power output σ_{power} and the blade pitch rate $\sigma_{\mathrm{pitch\_rate}}$ are minimized to mitigate power fluctuation and reduce actuator mechanical wear, respectively, capturing the critical trade-off between power quality and actuator usage.

Thus, the optimization problem captures the inherent compromise among structural load mitigation, power output and actuator preservation. Its goal is to find the Pareto-optimal controller parameters that define the best possible compromises between these conflicting demands.

D. NSGA-II Optimization Framework

The multi-objective optimization [12], [13] was performed using the NSGA-II algorithm via MATLAB's gamultiobj function. The optimization follows an iterative process as illustrated in Fig. 2. The process began by initializing a population of 200 individuals, with each candidate solution representing a pair of PI parameters (K_p, K_i) randomly generated within the predefined bounds. For each generation, the entire population was evaluated by running OpenFAST simulations with the candidate parameters to compute the three objective functions: blade root bending moments DEL, power standard deviation, and pitch rate standard deviation. These simulations were accelerated through parallel computation. Following evaluation, the algorithm performed non-dominated sorting to rank the solutions based on Pareto dominance and calculated the crowding distance to preserve diversity across the front. To create the next generation, tournament selection with a size of 4 was applied to choose parents, which were then recombined using intermediate crossover (with a fraction of 0.8) and perturbed via adaptive feasible mutation to maintain genetic diversity. This evolutionary loop continued until a maximum of 100 generations was reached, or the optimization stalled for 10 generations, or the change in the objective functions fell below a tolerance of 1e-3, at which point the final set of Pareto-optimal solutions was output. The total computational cost of this offline optimization was approximately 8 hours on a workstation equipped with an AMD Ryzen 9 9955HX 16-Core Processor and 32 GB RAM, with 16 cores used in parallel for OpenFAST simulations. Given that the tuning is performed entirely offline and the resulting Pareto-optimal PI parameters are fixed during real-time operation, this computational expense is reasonable and well justified by the achieved improvements in load mitigation and power quality.

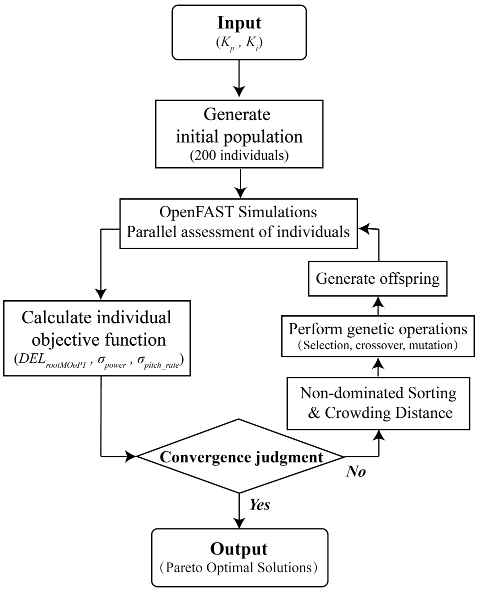

Fig. 2 Flowchart of the NSGA-II optimization framework for IPC PI parameter tuning

3. Results and Discussion

Following the optimization framework established in Section II, this section presents and analyzes the key outcomes. First, the Pareto front obtained from the NSGA-II optimization is examined to elucidate the fundamental trade-offs between load mitigation, power quality, and actuator usage. Subsequently, a detailed performance comparison is conducted between selected optimal strategies and the baseline collective pitch controller, evaluating their effectiveness across critical metrics including blade loads, platform motion, and pitch activity.

A. Pareto Front Analysis

The three-dimensional Pareto front obtained from the NSGA-II optimization vividly illustrates the inherent trade-offs among the three competing objectives: blade root load reduction (DEL), power quality (σ_{power}), and actuator preservation (σ_{pitch_rate}), as shown in Fig. 3. To facilitate a concrete analysis of these trade-offs, four representative optimal solutions were extracted from the front using distinct selection strategies, as visually summarized in the two-dimensional projection focusing on the DEL vs. σ_{pitch_rate} trade-off, as shown in Fig. 4. The corresponding PI controller gains (K_p and K_i) for these four strategies are listed in Table II. First, a balanced solution was identified by selecting the design point with the minimal normalized Euclidean distance to the ideal utopia point (where all objectives are simultaneously minimized), representing the best compromise. Subsequently, three extreme solutions were chosen by individually minimizing each objective function: the load-optimal solution (minimizing DEL), the power-optimal solution (minimizing σ_{power}), and the actuator-optimal solution (minimizing σ_{pitch_rate})). These four solutions collectively encapsulate the key performance characteristics along the Pareto boundary and will be used for detailed comparative performance evaluation in the following section.

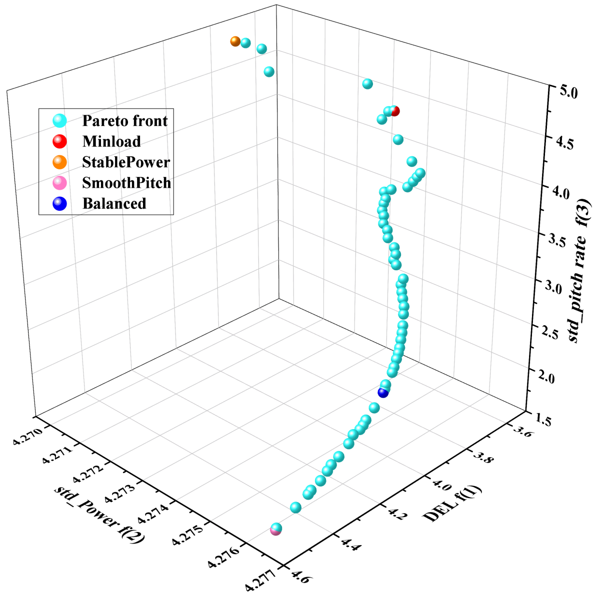

Fig. 3 Three-dimensional Pareto front

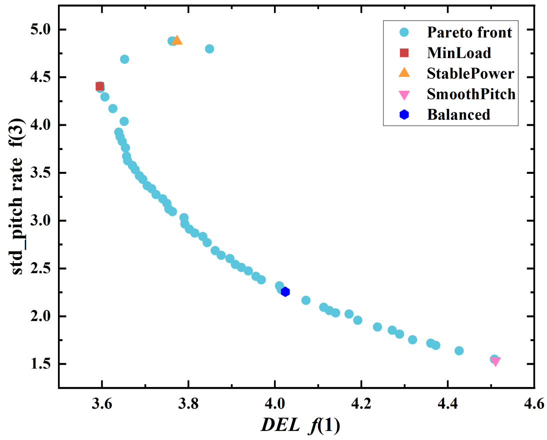

Fig. 4 Pareto front (*Pitch rate* vs $DEL_{rootMOoP}$)

Table II. - Optimized PI controller parameters for selected IPC strategies

SOLUTION TYPE	PARAMETERS	
	K_p	K_i
Balanced	2.58e-09,	1.07e-11
MinLoad	9.83e-09,	1.21e-10
StablePower	1.00e-08,	9.99e-10
SmoothPitch	1.23e-10	1.03e-11

B. Performance Comparison

Based on the 300-second time-domain simulation data, a comparative analysis between the baseline CPC and the four optimized IPC strategies reveals a distinct set of engineering trade-offs, demonstrating how distinct optimization priorities lead to measurably different operational profiles for the floating offshore wind turbine, as shown in Fig. 5 - Fig. 8.

The analysis begins by establishing the performance of the baseline CPC strategy, which is characterized by moderate pitch actuator activity (standard deviation of 1.985°) but results in the highest dynamic load fluctuations on the blade root (standard deviation of 8356.0 $kN{\cdot}m$) and a significant mean platform pitch of 1.739°. This serves as the benchmark against which the optimized IPC strategies demonstrate their specialized advantages and inherent compromises.

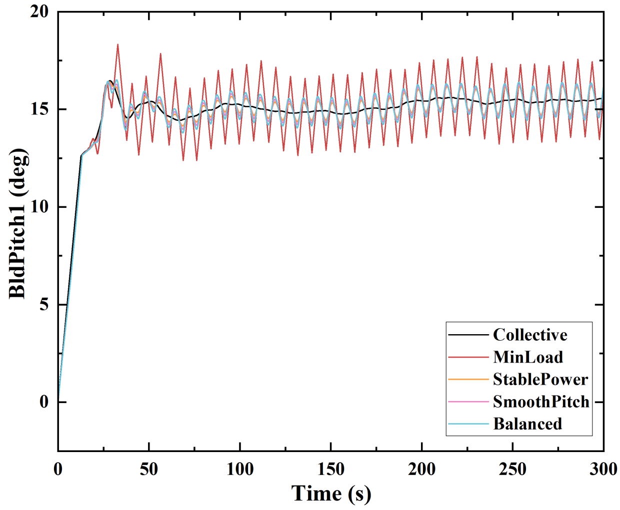

Fig. 5 Comparison of blade pitch angles under different control strategies

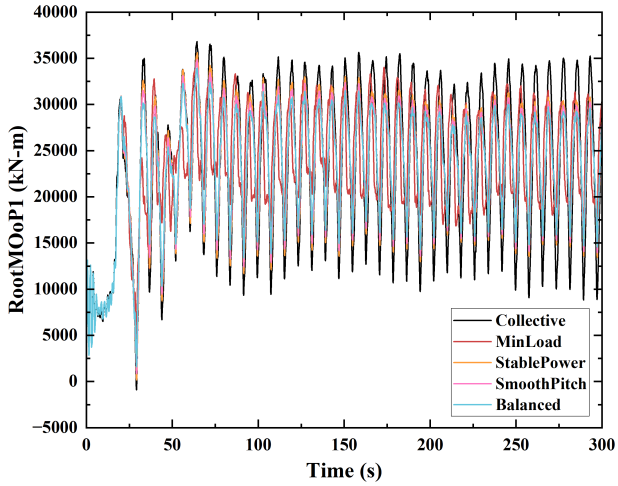

Fig. 6 Blade root out-of-plane bending moment responses under different control strategies

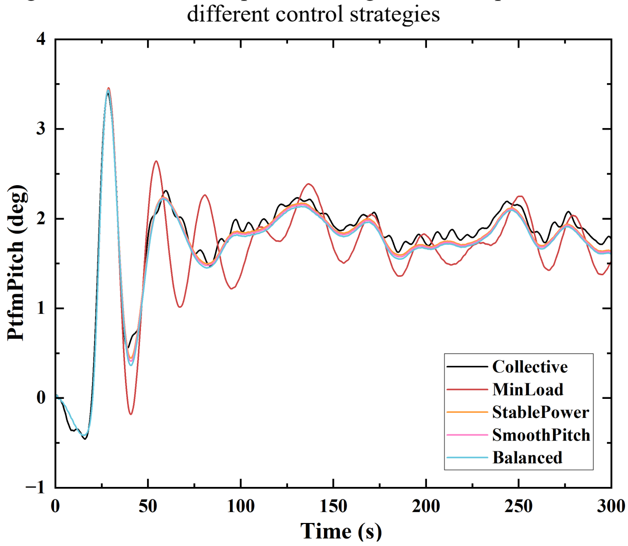

Fig. 7 Time history of platform pitch motion under different control strategies

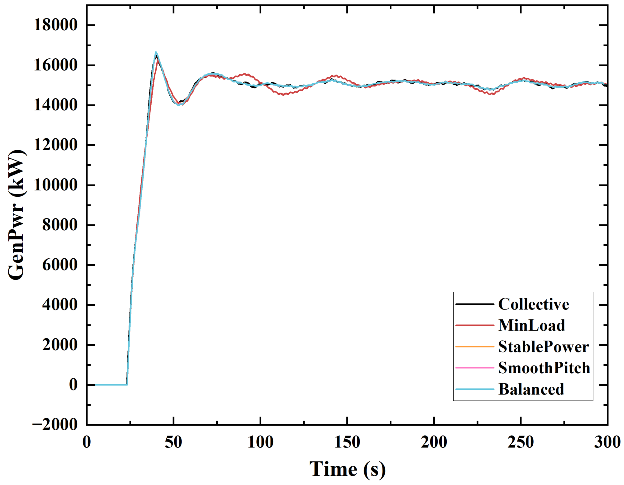

Fig. 8 Generator power output under different control strategies

The pitch angle activity discussed in Fig. 5 is shown for Blade 1. This representation is appropriate because the simulated scenario involves a low-turbulence wind field. Consequently, the resulting pitch signals for the three blades exhibit consistent amplitude and a fixed phase relationship: the trajectories for Blades 2 and 3 are identical to that of Blade 1 but with constant phase offsets of 120° and 240°, respectively. Therefore, the time series for a single blade fully characterizes the IPC actuation pattern for the entire rotor in the present study.

The MinLoad strategy, explicitly designed for minimal fatigue loads, validates its purpose by achieving the most substantial suppression of blade root load fluctuations, reducing the standard deviation by 25.8% to 6199.5 $kN{\cdot}m$. Fig. 6 visually corroborates this with its significantly reduced amplitude of load variations. This dramatic improvement in dynamic load mitigation is achieved through the most aggressive pitch control actions among all strategies, as evidenced by a 17.7% increase in the standard deviation of the pitch rate. Consequently, the most aggressive pitch actions of this strategy, while reducing blade loads, impose significant aerodynamic-excitation on the entire floating system. This control-induced motion is directly reflected in the platform dynamics, resulting in the largest amplitude of pitch angle variation among all strategies, as can be observed in the platform pitch time series of Fig. 7, where the MinLoad trajectory exhibits the most pronounced oscillations. In stark contrast, the SmoothPitch strategy prioritizes actuator longevity by minimizing pitch rate variability. While it successfully limits pitch action to a level only 5.7% above the baseline, yielding the smoothest pitch angle trajectory in Fig. 5. Nevertheless, it secures a considerable 23.2% reduction in load fluctuations and a 3.9% decrease in mean platform pitch, demonstrating that even a restrained IPC implementation delivers tangible structural and stabilization benefits.

The StablePower strategy presents a particularly insightful case. Its core objective was to minimize power fluctuations (σ_{power}); however, as illustrated in Fig. 8, the generator power output time series for all strategies are nearly superimposed. Quantitatively, the standard deviation of generator power remains nearly identical (varying by less than 0.3%) across all strategies, including the baseline. This critical finding reveals that within the defined operational envelope and optimization constraints, power quality was not the primary limiting factor differentiating the Pareto solutions. Instead, the optimization process traded performance almost entirely between load reduction and actuator duty. Therefore, the outcome of the StablePower strategy is a well-balanced compromise between the two active trade-offs: it achieves a 19.3% reduction in load fluctuations while maintaining pitch activity very close to the SmoothPitch strategy, making it a conservative yet effective option.

Ultimately, the Balanced strategy, selected for its optimal compromise on the three-dimensional Pareto front, emerges as the most comprehensively proficient solution. It does not merely average the performance of the other strategies but finds a superior equilibrium point. It delivers the strongest overall load mitigation, reducing the blade root bending moment standard deviation by 27.6%—the best result among all strategies. This is evident in Fig. 6, where the Balanced strategy's load signal shows the most effective amplitude suppression. It accomplishes this while increasing pitch action by only 6.7%, a far more modest cost than the MinLoad strategy. Furthermore, it provides excellent platform stabilization, reducing the mean pitch angle by 5.0%, which is second only to the MinLoad strategy.

In summary, the data narrates a clear progression from a specialized, high-effort solution (MinLoad) to a refined, high-efficiency solution (Balanced), with intermediate strategies (StablePower, SmoothPitch) providing tailored options for specific operational priorities, all while conclusively demonstrating the universal superiority of optimized IPC over conventional collective pitch control for floating wind turbines.

4. Conclusion

This study has successfully addressed the critical challenge of parameter tuning for Individual Pitch Control (IPC) in floating offshore wind turbines by formulating and solving a multi-objective optimization problem. The core of the work involved applying the NSGA-II algorithm to find Pareto-optimal sets of the PI controller gains (K_p, K_i) that explicitly balance the conflicting objectives of blade root fatigue load reduction, power quality stabilization, and pitch actuator duty minimization. The key finding confirms that optimized IPC universally and significantly outperforms standard collective pitch control. All optimized strategies dramatically reduced the dynamic fluctuation of the blade root out-of-plane bending moment (standard deviation reduced by 19.3% to 27.6%) and improved platform pitch stability, directly targeting the primary sources of structural fatigue in floating systems. Future work may focus on validating these optimized gains under a broader set of turbulent wind and irregular wave conditions and exploring online adaptive mechanisms to maintain optimal performance across the turbine's entire operational envelope.

Acknowledgement

This work has been partially supported by the Spanish Ministry of Science and Innovation under the projects MCI/AEI/FEDER number PID2021-123543OB-C21 and PID2024-155653OB-C21.

References

[1] J. G. Njiri and D. Söffker, "State-of-the-art in wind turbine control: Trends and challenges," *Renew. Sustain. Energy Rev.*, vol. 60, pp. 377–393, Jul. 2016, doi: 10.1016/j.rser.2016.01.110.

[2] D. Bai, B. Wang, Y. Li, and W. Wang, "Study on load reduction and vibration control strategies for semi-submersible offshore wind turbines," *Sci. Rep.*, vol. 15, p. 1148, Jan. 2025, doi: 10.1038/s41598-025-85476-3.

[3] H. Namik and K. Stol, "Individual blade pitch control of floating offshore wind turbines," *Wind Energy*, vol. 13, no. 1, pp. 74–85, 2010, doi: 10.1002/we.332.

[4] A. Eskandari, R. Vatankhah, and E. Azadi, "Optimization of wind energy extraction for variable speed wind turbines using fuzzy backstepping sliding mode control based on multi objective PSO," *Ocean Eng.*, vol. 285, p. 115378, Oct. 2023, doi: 10.1016/j.oceaneng.2023.115378.

[5] S.-J. Jiang, S.-C. Chu, F.-M. Zou, J. Shan, S.-G. Zheng, and J.-S. Pan, "A parallel Archimedes optimization algorithm based on Taguchi method for application in the control of variable pitch wind turbine," *Math. Comput. Simul.*, vol. 203, pp. 306–327, Jan. 2023, doi: 10.1016/j.matcom.2022.06.027.

[6] G. Li and T.-C. Chen, "Multi-objective mathematical model for optimal wind turbine placement in wind farm under uncertainty," *J. Eng. Res.*, vol. 13, no. 4, pp. 3249–3259, Dec. 2025, doi: 10.1016/j.jer.2024.09.014.

[7] L. Xiaoqing, D. Haiying, L. Hongwei, L. Mingxue, and S. Zhiqiang, "Optimization Control of Front-End Speed Regulation (FESR) Wind Turbine Based on Improved NSGA-II," *IEEE Access*, vol. 7, pp. 45583–45593, 2019, doi: 10.1109/ACCESS.2019.2908995.

[8] C. Allen *et al.*, "Definition of the UMaine VolturnUS-S reference platform developed for the IEA wind 15-megawatt offshore reference wind turbine," National Renewable Energy Lab.(NREL), Golden, CO (United States); Univ. of …, 2020. doi: 10.2172/1660012.

[9] K. Selvam, S. Kanev, J. W. van Wingerden, T. van Engelen, and M. Verhaegen, "Feedback–feedforward individual pitch control for wind turbine load reduction," *Int. J. Robust Nonlinear Control*, vol. 19, no. 1, pp. 72–91, 2009, doi: 10.1002/rnc.1324.

[10] C. Serrano, J.-E. Sierra-Garcia, and M. Santos, "Hybrid Optimized Fuzzy Pitch Controller of a Floating Wind Turbine with Fatigue Analysis," *J. Mar. Sci. Eng.*, vol. 10, no. 11, p. 1769, Nov. 2022, doi: 10.3390/jmse10111769.

[11] M. T. Todinov, "Necessary and sufficient condition for additivity in the sense of the Palmgren–Miner rule," *Comput. Mater. Sci.*, vol. 21, no. 1, pp. 101–110, May 2001, doi: 10.1016/S0927-0256(00)00221-4.

[12] F. Alonso Zotes and M. Santos Peñas, "Multi-criteria genetic optimisation of the manoeuvres of a two-stage launcher," *Inf. Sci.*, vol. 180, no. 6, pp. 896–910, Mar. 2010, doi: 10.1016/j.ins.2009.11.001.

[13] L. Ren *et al.*, "Mitigation of vibrations and its optimization in a large floating wind turbine across different typhoon stages," *Ocean Eng.*, vol. 330, p. 121287, Jun. 2025, doi: 10.1016/j.oceaneng.2025.121287.